LUNAR NETWORK TRACKING ARCHITECTURE FOR LUNAR FLIGHT

Shane B. Robinson*

A trade study was conducted with the objective of comparing and contrasting the radiometric navigation performance provided by various architectures of lunar-based navigations assets. Architectures considered consist of a compliment of two beacons located on the lunar surface, and two orbiting beacons that provide range and range-rate measurements to the user. Configurations of these assets include both coplanar and linked constellations of frozen elliptic orbiters and halo orbiters. Each architecture was studied during the lunar-approach, lunar-orbit, and landing phases of a South Pole lunar sortie mission. Navigation filter performance was evaluated on the basis of filter convergence latency, and the steady state uncertainty in the navigation solution. The sensitivity of the filter solution to Earth-based tracking augmentation and availability of range measurements was also studied. Filter performance was examined during the build up of the lunar-based navigation system by exploring different combinations of orbiting and surface-based assets.

1 INTRODUCTION

The objective of the work outlined in this document is to conduct a parametric trade intended to evaluate some proposed constellations of moon-orbiting navigation and communication beacons. These orbiting beacons are intended to support the lunar missions of NASA's Constellation program. This study is sponsored by the flight performance systems integration group at JPL (FPSIG), whose work is funded by the NASA Constellation program office. The work outlined in this report will focus on investigating lunar network aided navigation performance during near lunar phases of baseline missions proposed by the Constellation program.

The proposed orbiting beacons use radiometric measurements to measure the range and/or range-rate of the spacecraft. Figure 1 shows the three basic types of radiometric measurements considered.

Range measurements are produced by measuring the time-of-flight of the signal. Range measurements can be produced generated using both one and two way strategies. One-way measurements are subject to timing errors caused by inaccuracies in oscillator/clock on board the receiver. Two-way range measurements measure the time-of-flight of a signal that is coherently transponded by the spacecraft. The two-way strategy offers much improved measurement quality by eliminating the substantial oscillator error of the spacecraft.

Range-rate measurements produced by measuring the Doppler shift of the signal. For the one-way case these measurements are also corrupted by the inaccuracies in the oscillator. The two-way avoids these difficulties by measuring the beat frequency of the coherent transponded signal superimposed onto the original signal.

Errors in the transmitter clock can affect the accuracy of the measurement. Typically the clock errors from the receiver dominate the clock errors. Consequently, two-way measurements are significantly more precise than one-way measurements.

Three-way measurements is essentially a one-way measurement combined with two-way measurement. One attractive feature of three-way measurements is that they require no additional modification to a two-way capable spacecraft, but do require that the second station have an accurate clock that is calibrated with the primary station. While one- and two-way measurements only provide information along the line of sight, three-way measurements provide information in the plane defined by the two ground stations and the spacecraft. This constitutes a significant increase in information content in three-way Doppler measurements when compared to one- and two-way.

All of these measurement strategies can be implemented using ground stations and/or orbital communication/navigation relays. This study will evaluate the navigation performance for a proposed configuration of moon-orbiting beacons that provide one- and two-way measurements to the Orion-Altair spacecraft when, it is in the vicinity of the moon.

*Graduate Student, Mechanical and Aerospace Engineering, Utah State University, 4130 Old Main Hill, Logan, Utah, 84322-4130, USA

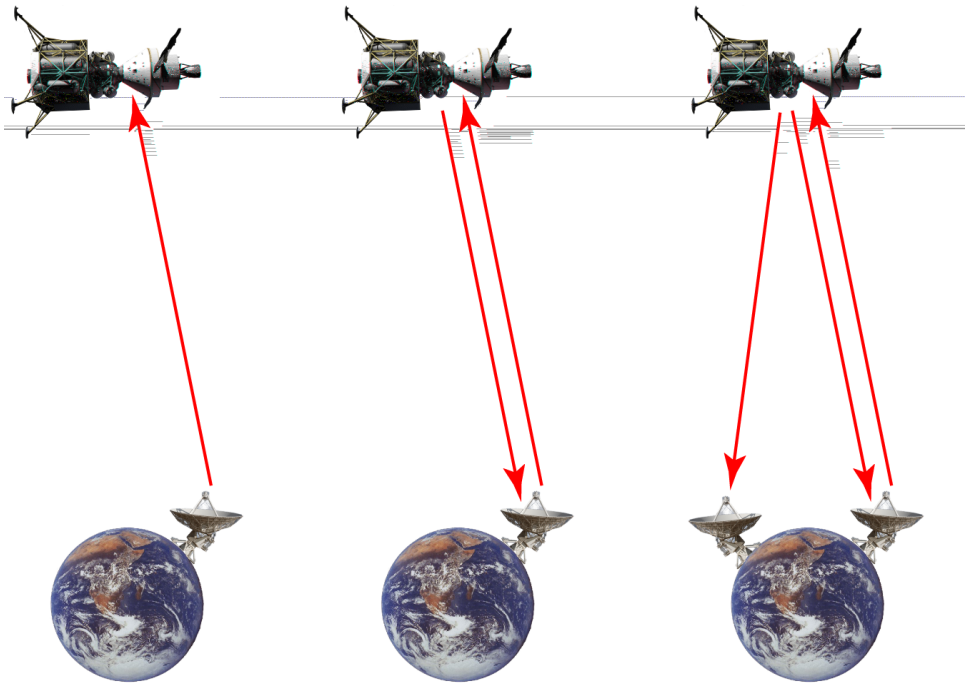

Figure 1. Radiometric measurement strategies: (a) one-way, (b) two-way, and (c) three-way.

Last summer a similar study was conducted by the FPSIG and the author to evaluate the sensitivity of navigation performance during the lunar orbit phases of the mission with respect to the Earth based ground station (EBGS) tracking architecture. The study conducted last summer considered three configurations of the EBGS, which are shown in Figure 2.

The Apollo Manned Space Flight Network (MSFN) - This is the tracking systems used during the Apollo lunar missions. It consisted of 12 stations placed around the Earth. The performance of this large network is compromised by the proximity of many of these stations to each other, and/or the equator. At the conclusion of the Apollo program this large network was no longer needed. As a result, presently only the three stations that constitute the deep space network are currently available for lunar tracking purposes.

The Deep Space Network (DSN) - This network consists of the stations from the MSFN located at Goldstone, California; Madrid, Spain; and Canberra, Australia. Together these stations constitute the currently available network for deep space tracking. The DSN is the tracking network used by the majority of spacecraft outside of Earth orbit.

Integrated Design and Analysis Cycle 4B (IDAC-4B) - This proposed ground tracking station configuration consists of the DSN augmented by 3 additional stations. The stations proposed to augment the DSN are located in Santiago, Chile; Hartebestock, South Africa; and Usuda, Japan. These stations are intended to be used as secondary stations to the DSN. As secondary stations they well be receive only stations for three-way Doppler. These stations are arranged at nearly the same longitude as the existing DSN stations, but at opposing latitudes. This establishes a north-south tracking baseline and enhances the existing east-west tracking baseline of the DSN.

This prior study has two principle results. First, the navigation filter performed nearly as well (in some cases better) with the IDAC-4B network as it did with the MSFN, however the DSN offered clearly inferior performance. This indicates the proposed IDAC-4B network would meet the performance requirements. Second, the increased information content for three way Doppler measurements allows the filter to rapidly converge to a much more accurate solution than is possible without three-way measurements.

Since last summer FPSIG has conducted more studies evaluating the performance of the same earth based tracking

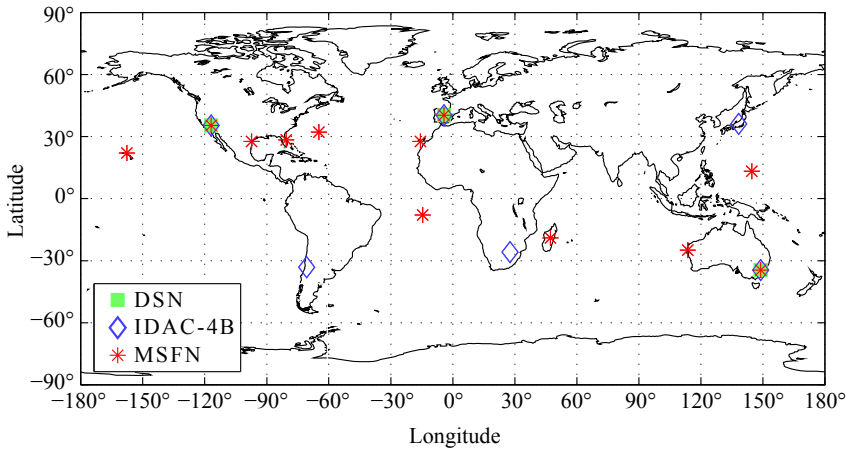

Figure 2. The geographic configurations of the EBGS architectures considered.

networks for supporting a ballistic atmospheric reentry[1]. These studies concluded that the IDAC-4B can provide nearly the same level of tracking support that the MSFN could provide. Studies by the FPSIG group also showed that the unfortunate lack of acceleration knowledge (FLAK) causes the navigation filter to rapidly loose certainty in its solution.

2 PROPOSED LUNAR NETWORK

The lunar architecture team (LAT) has proposed a network of lunar-based navigations assets shown in Figure 3. The LAT-2 network consists of two moon-orbiting lunar relay satellites (LRS), and two ground based lunar communications terminals (LCT). These four assets all serve as radiometric navigation beacons for the users in lunar orbit as well as the users on surface.

The LAT-2 network is intended to meet all of the navigational requirements of the Constellation program with only one LRS and one LCT. The second LRS and LCT provide a layer of redundancy in addition to offering improved navigation performance. It is anticipated that, the minimal compliment of assets will be used during the build-up phase of the LN before all of the assets are operational. The single LRS/LCT situation might also be encountered in the event of an asset failure.

This study will consider various LRS constellations. The constellations are composed of two classes of orbiters: 1) frozen elliptic orbiters, and 2) halo orbiters.

2.1 Frozen Elliptic Orbiters

Ely[2, 3] has found a family of inclined elliptic orbits that are boundedly stable in e, eccentricity, and ω^{op}, argument of periapse with respect to the lunar orbital plane. and provide coverage of the south pole. The behavior or the mean argument of periapse with respect to the lunar orbital plane is defined by

$$e^2\left(1-\frac{5}{2}\sin^2\left(i^{\text{op}}\right)\sin^2\left(\omega^{\text{op}}\right)\right)=\beta \tag{1}$$

where β is a constant, and ω^{op} librates about $\omega^{\text{op}}=90^\circ, 270^\circ$. The eccentricity of the orbit librates about the value given by

$$e^2=1-\frac{5}{3}\cos^2\left(i^{\text{op}}\right) \tag{2}$$

The trajectory of e is defined by the equation

$$\left(1-e^2\right)\cos^2\left(i^{\text{op}}\right)=\alpha \tag{3}$$

where α is a constant of motion.

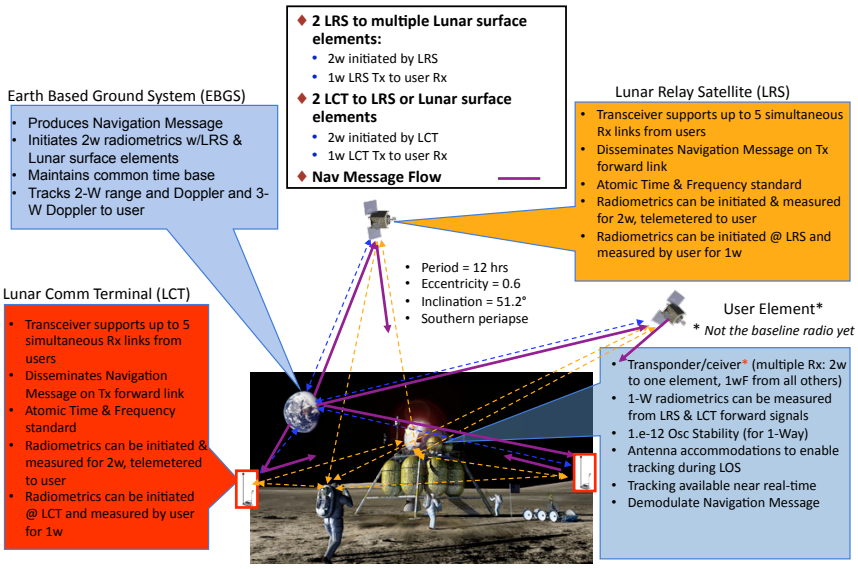

Figure 3. A schematic of the proposed LAT-2 configuration of the LN.[1].

An orbit was selected that use both of these phenomena to produce an orbit with desirable stability characteristics. The semimajor axis of the orbit is selected so that to meet the altitude constraints. Initial values for the orbit used in this study are shown in table 1.

Table 1. Initial values of the orbital elements for the frozen elliptic orbits.

Orbital Element	Value
Semimajor axis, a	6142.6 km
Eccentricity, e	0.6
Inclination, i^{op}	51.1655°
Longitude of Ascension, Ω^{op}	0
Argument of Periapse, ω^{op}	90°

The four constellations of frozen elliptic orbiters are shown in figure 4. These constellations include: 1) a singe orbiter with southern apoapse, 2) two coplanar orbiters with southern apoapse, 3) two orbiters with southern apoapse and orthogonal orbital planes, and 4) one orbiter with a northern apoapse, one with a southern apoapse and orthogonal orbital plane. For all the cases with two elliptic orbiters the orbiters are separated by 180° of mean anomaly.

For orbital planes with the same inclination to be orthogonal the following adjustment must be made to the right ascension of the ascending node.

$$\cos\left(\Delta\Omega^{\text{op}}\right) = -\cot\left(i^{\text{op}}\right) \tag{4}$$

This equation requires that $\frac{\pi}{4} \leq i^{\text{op}} \leq \frac{3\pi}{4}$. The details of this equations development can be found in Appendix **??**.

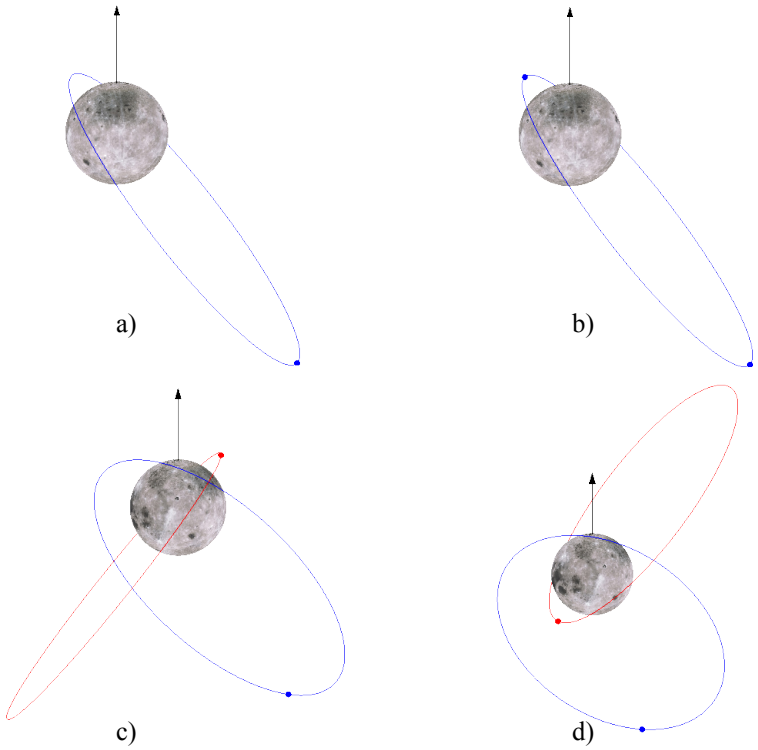

Figure 4. Constellations of frozen elliptic orbiters. The arrow indicates the lunar north pole. a) a single orbiter with souther apoapsis, b) two coplanar orbiters with southern apoapsis, c) orthogonal planes with southern apoapsis, d) orthogonal planes with souther and northern apoapsis.

2.2 Halo Orbiters

Two halo orbiter constellations[4, 5, 6, 7] were also considered. Figure shows a halo orbit. The halo orbits used in this study were chosen using the methodology outlined by Parker[7, 4].

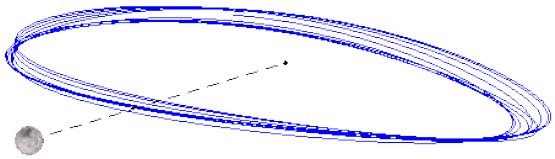

Figure 5. L_2 Halo orbit trajectory in the synodic frame. The dashed line indicates the location of the L_2 point relative to the moon.

3 METHODS

This study examined navigation performance for phases shown in table 2 for flight in the vicinity of the moon. Currently, this study focuses on CFP1P, a conceptual flight profile for a lunar south pole mission. The profile of CFP1P is shown in figure 6. The analysis conducted includes the approach, lunar orbit, and landing phases of CFP1P.

3.1 Tradespace

In addition to the six constellations considered the effect of other factors on navigation performance was considered. The performance of each constellation with and without the support of the IDAC-4B network was compared. The effect

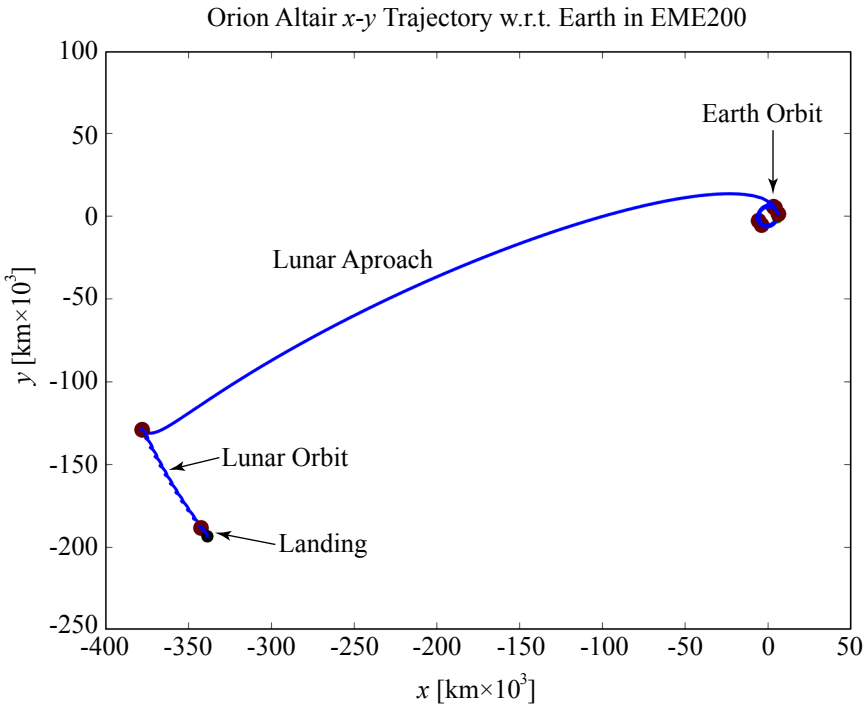

Figure 6. The profile of CFP1P.

of range measurements on the navigation solution was also evaluated. For landing cases the relative right ascension of the constellations with respect to the lander will also be varied.

3.2 Software

These trade studies have been conducted using JPL's Lumina software. Lumina is a lunar navigation architecture tool developed at JPL that has the capability to perform all of the analysis outlined in this report. Lumina propagates a trajectory for the entire mission, simulates all of the measurements, then uses a U-D Kalman Filter to produce the navigation solution. Recently this tool has been upgrades to include the effects of execution errors during maneuvers. This insures that the navigation solution reflects the uncertainty in the trajectory caused by the imperfect execution of maneuvers. Lumina also includes the effect that FLAK has on the filter solution by varying the process noise on the filter to simulate the wake and sleep periods of the crew. A example of the navigation solution produced by Lumina is shown in figure 7.

Last summer a trade spawning application was created. Since then members of FPSIG have upgraded the trades spawner application to efficiently run simultaneously on several nodes of a cluster. Additional upgrades have been made recently that give the trade-spawner the capability to automatically generate reports using LaTeX. These improvements have greatly reduced the time required to execute a study once the study has been setup.

4 RESULTS

The results obtained for lunar approach, and lunar orbit, are shown in table 3. Analysis of this data along time histories of the navigation uncertainty

4.1 Lunar Approach

A valuable metric for evaluating the navigation performance during lunar approach is the variance in the altitude based on the knowledge errors, and execution errors at the final trajectory correction maneuver. The variance in the

Table 2. Near-Lunar trajectory phases considered in this analysis.

Flight Phase	Starting Epoch	Ending Epoch	Tracking Networks
Lunar Approach	LOI-1day	LOI	LN with and without EBGS
Lunar Orbit	LOI	PDI	LN with and without EBGS
Lunar Landing	DOI	Landing	LN only
Surface Operations	—	—	LN with and without EBGS

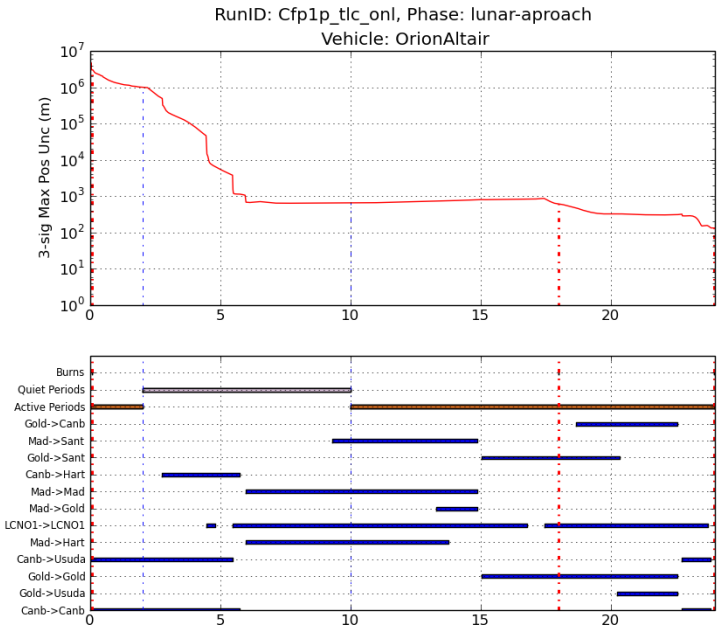

Figure 7. Lumina output for the lunar approach section of the trajectory for a single southern apoapsis LRS with IDAC-4B support and range measurements.

altitude for each configuration is shown in figure 8.

There are several interesting results can be observed in this figure:

- Augmenting the EBGS with any configuration of the LN network produces nearly double the navigation performance of the EBGS alone. When the EBGS is available the solution shows little sensitivity to the configuration of the lunar tracking network. The particular configuration of the lunar network is not as important as the existence of a lunar network.
- Without the aid of the EBGS the halo orbiters cannot adequately support lunar approach. This situation results in significant probabilities of lunar impact, which are unacceptable.
- When the EBGS is available, range measurements do not substantially improve the solution provided by Doppler only. When the EBGS is not available the addition of range measurements to Doppler can improve the solution by a factor of nearly two. However, this improvement requires that two orbiting beacons be available. The two orbiting beacons are needed to remove the range bias.
- The LCTs do not play a significant role during lunar approach. The spacecraft is unable to access the measure-

Table 3. Results for the lunar approach and lunar orbit phases of the mission.

Range on/Range off	Lunar Approach LOI-24hrs➔LOI			Lunar Orbit LOI➔PDI		
Lunar Network Configuration	Latency [hr]	Position Error [km]	Velocity Error [m/s]	Latency [min]	Position Error [m]	Velocity Error [m/s]
Single Elliptic Orbiter						
Single Southern Apoapsis						
EBGS on	2/2	0.6/0.6	0.02/0.02	3/3	10/10	0.02/0.02
EBGS off	2.5/3	100/160	3/5	80/80	60/60	0.03/0.03
Coplanar Elliptic Orbiters						
South/South Apoapsis						
EBGS on	3/10	0.4/0.8	0.06/0.1	3/3	10/20	0.02/0.02
EBGS off	4/10	2.5/10	0.3/0.8	25/25	30/30	0.03/0.03
Orthagonal Elliptic Orbiters						
South/South Apoapsis						
EBGS on	1.5/1	0.16/1.0	0.03/0.05	3/10	12/20	0.02/0.02
EBGS off	1.5/2	1.6/30	0.1/0.3	80/80	25/40	0.02/0.03
North/South Apoapsis						
EBGS on	1.5/1	0.1/1.0	0.02/0.04	3/10	20/20	0.03/0.02
EBGS off	1.5/2	1.0/30	0.1/0.4	65/65	25/25	0.03/0.03
Halo Orbiters						
Single Halo						
EBGS on	2/5	0.6/1.0	0.02/0.05	3/3	4.0/4.0	0.01/0.01
EBGS off	-	4000/5000	63/100	110/110	10/20	0.01/0.01
Double Halos						
EBGS on	4/10	0.4/5.0	0.006/0.06	3/10	3.0/4.0	0.005/0.005
EBGS off	-	250/2500	5.0/20	10/10	8.0/8.0	0.01/0.01

ments from the LCT during lunar approach because of the range constraint on the LCT, and limited visibility that the LCT has from the lunar south pole.

- Filter latency is driven by the geometric diversity of the measurements. Thus, configurations with orthogonal planes proved favorable characteristics. However, this improvement is a relatively minor. When compared with the large benefit provided by the availability of the EBGS.

4.2 Lunar Orbit

The navigation uncertainly was comparable for nearly all of the cases that were run.

- The halo orbiters provided a marginal improvement in the navigation uncertainly. It is believed that this improvement can be attributed to the fact that the higher altitude of the halo orbiter enables the spacecraft to receive more measurements.
- Convergence latency is driven by the EBGS. When the EBGS is available, the convergence time is <10 min. In the absence of the EBGS most lunar networks require nearly an entire orbit to converge to the final solution. The only exception is the double halo orbiters which provide a convergence latency of only 10 min.
- When the EBGS is available the solution is <15 meters. Without the EBGS the solution <30 meters. This represents a improvement by a factor of two.
- The solution is not sensitive to the availability of range measurement. Doppler measurements alone provide nearly the same solution as Doppler and range measurements.

4.3 Lunar Landing

The first metric considered during landing was the delivery errors at powered decent initiation (PDI). It was discovered the the delivery errors at PDI changed very little depending on the specific case examined. The position

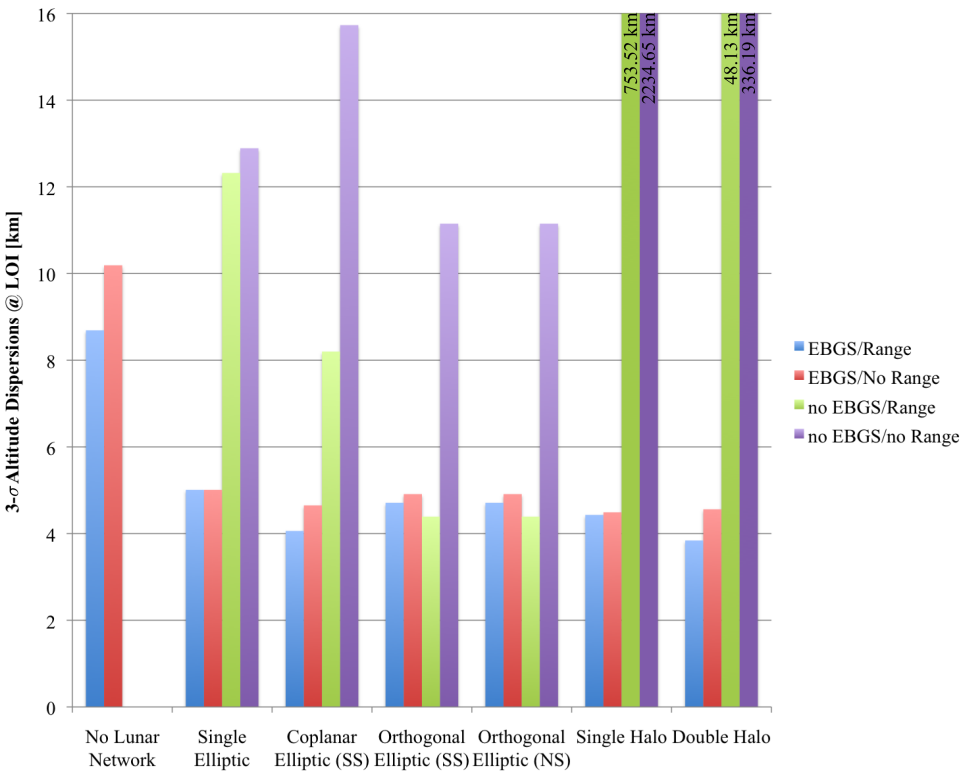

Figure 8. The delivery error in the altitude channel for lunar orbit insertion.

uncertainly just prior to performing the de-orbit burn is so small (<10 meters) that they can be neglected. Thus the delivery errors at PDI are only a function of the execution errors the the de-orbit burn and the process noise that perturbs the system. Figure 9 shows the delivery errors at PDI. Analysis of the data also indicated that the knowledge errors at PDI are almost driven by the altimeter and are nearly constant. The vary depending on the configuration of the lunar network.

The data also showed that once the LCT comes into view it dominates the navigation solution. Future studies need to be conducted to evaluate the performance when the LCT is not available.

5 CONCLUSIONS

All of the effects indicated above are effects of the dynamics of the system. Good solutions are present when either the user spacecraft or the orbiting beacon are subject to relatively large levels of acceleration. These relatively large levels of acceleration serve to produce geometric diversity in the radiometric measurements. The need for this geometric diversity is driven by the unfortunate lack of acceleration knowledge (FLACK) associated with crewed spacecraft. FLACK is caused by the activity of the crew, and results in small accelerations that are too small to accurately detect with available accelerometer and gyroscope technology. However, these small random accelerations can have large effects on the location of the trajectory at a future time. FLACK has an unknown nature, and the navigation filter must account for FLACK by using large levels of process noise. These large levels of process noise continually introduce uncertainty into the filter estimate. The unidirectional nature of the radiometric measurements causes difficulty in resolving the estimate if the measurements have little or no geometric diversity. In other words, when the radiometric measurement direction is relatively stagnant in time, the filter is unable to return a estimate with a reasonable level of confidence. Thus, for crewed spacecraft on trans-lunar trajectories it is suggested that radiometric measurements with geometric diversity need to be available at frequent intervals to insure the fidelity of the navigation filter solution by inhibiting the growth of uncertainty in the navigation filter estimate.

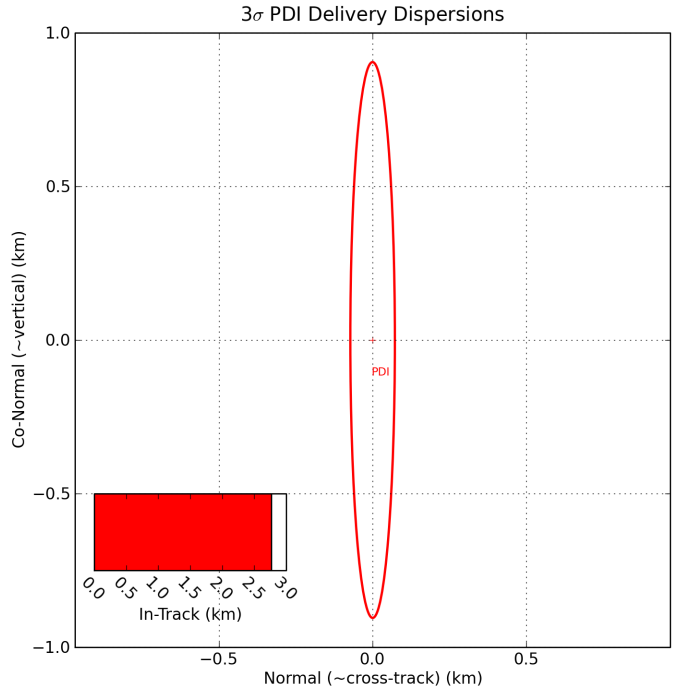

Figure 9. The delivery errors at PDI.

REFERENCES

[1] T. A. Ely and M. Abrahamson, "Lunar Navigation and Tracking Architecture IDAC-4B Results," Presentation to CxAWG, NASA, December 2008.

[2] T. A. Ely, "Stable Constellations of Frozen Elliptical Inclined Lunar Orbits," *The Journal of the Astronautical Sciences*, Vol. 53, July-September 2005, pp. 301–316.

[3] T. A. Ely and E. Lieb, "Constellations of Elliptical Inclined Lunar Orbits Providing Polar and Global Coverage," *The Journal of the Astronautical Sciences*, Vol. 54, January-March 2006, pp. 53–67.

[4] J. S. Parker, *Low-Energy Ballistic Transfers*. PhD thesis, University of Colorado, 2007.

[5] K. Hill, J. S. Parker, G. H. Born, and N. Demandante, "A Lunar L_2 Navigation, Communication, and Gravity Mission," *AIAA/AAS Astodynamic Specialist Conference and Exhibit*, No. AIAA 2006-6662, Keystone, Colorado, 2006.

[6] D. J. Grebow, M. T. Ozimek, K. C. Howell, and D. C. Folta, "Mulibody Orbit Achitectures for Lunar South Pole Coverage," *Journal of Spacecraft and Rockets*, Vol. 45, March-April 2008, pp. 344–358.

[7] J. S. Parker and G. H. Born, "Direct Lunar Halo Orbit Transfers," *The Journal of the Astronautical Sciences*, accepted for publication 2009.